Applying Raman micro-spectroscopy to evaluate the effects of nutrient cations on alkane bioavailability to *Acinetobacter baylyi* ADP1

Hanbing Li[a,b], Dayi Zhang[d,a], Jun Luo[b], Kevin C Jones[a,b,*] and Francis L Martin[c,*]

[a] Lancaster Environment Centre, Lancaster University, Lancaster LA1 4YQ, UK

[b] State Key Laboratory of Pollution Control and Resource Reuse, School of the Environment, Nanjing University, Nanjing 210023, China

[c] School of Pharmacy and Biomedical Sciences, University of Central Lancashire, Preston PR1 2HE, UK

[d] School of Environment, Tsinghua University, Beijing 100086, China

***Corresponding author**

Prof Kevin C. Jones

Lancaster Environment Centre, Lancaster University, Lancaster LA1 4YQ, UK

Tel.: +44 (0)1524 510230

Email: k.c.jones@lancaster.ac.uk

Prof Francis L. Martin

School of Pharmacy and Biomedical Sciences, UCLan, Preston, PR1 2HE, UK

Tel.: +44 (0)1772 896482

Email: dungar.martin@gmail.com

Abstract

Contamination with petroleum hydrocarbons, such as crude and mineral oils, can cause extensive damage to ecological systems. On oil contaminated sites, alkanes are major components; many indigenous bacteria exhibit the ability to access and/or degrade alkanes. However, their ability to do so is affected by external properties of the soil, including nutrient cations which can enhance or reduce their performance. This study therefore used Raman micro-spectroscopy techniques to study how nutrient cations affect alkanes' bioavailability to *Acinetobacter baylyi* ADP1 (a known degrader). Following treatment with Na, K, Mg and Ca at 10 mM, *A. baylyi* ADP1 was exposed to 7 n-alkanes (decane, dodecane, tetradecane, hexadecane, nonadecane, eicosane and tetracosane) and 1 alkane mixture (mineral oil). Raman spectral alterations identified from multivariate analysis indicated that bacterial availability of alkanes varied with carbon chain lengths and additional cations altered the bacterial response to n-alkane molecules. Sodium significantly increased the bacterial affinity towards short-chain alkanes (decane and dodecane), and K and Mg enhanced the bioavailability of medium-chain alkanes (tetradecane and hexadecane). In contrast, the bacterial response was inhibited by Ca for all alkanes. Similar results were observed in the treatment of mineral oil. Our study employed a novel Raman spectral assay to offer a deep insight into how nutrient cations affect bioavailability of alkanes, suggesting nutrient cations present in natural environments can play a key role to influence the harmful effects of such contaminants and could be optimised to enhance a bioremediation strategy.

1. Introduction

Rapid industrial development has caused the increasing use of petroleum hydrocarbons and their derivatives, such as crude oil and mineral oil. From the 1960's, more than 40 large oil spill incidents have been reported, *e.g.*, the Deepwater Horizon oil spill in Gulf of Mexico, the Xingang oil spill in Dalian, and the Exxon Valdez oil spill in Prince William Sound.[1-4] The release of hydrocarbons into the environment can result in extensive damage to natural ecological systems and serious threats to human health.[5-8] Oil spill accidents and relevant contaminated sites have therefore received considerable attention in recent decades. Biosensor and bioremediation methods are deemed as an environmentally friendly strategy to monitor and remove petroleum hydrocarbons from the environment.[9-13] Since alkanes are the main components of hydrocarbon contamination, whole-cell bioreporters have been used to evaluate bioavailability and bioaccessibility. Some have even been applied practically in the field, but low reproducibility has limited their use for alkane monitoring.[4,13] Numerous bacterial species show high hydrocarbon affinity in natural environments and can have sensitive responses to the bioavailable fractions of relevant alkanes.[14,15] However, environmental physicochemical conditions and nutrient deficiencies can limit bacterial activities, which consequently affect their behaviour towards alkanes.[16,17] Because bacterial selection and accumulation is significantly related to the bioavailability of alkanes,[18] it is necessary to understand how nutrients influence bacterial behaviours.

At hydrocarbon contaminated sites, bacterial cells have to collect and/or accumulate their surrounding alkane molecules.[18] The bioavailable alkane affects the sensory systems of bacterial cells, including selection, accumulation and/or utilization of alkanes.[19] Briefly, bacteria's sensory system consists of methyl-accepting chemotaxis protein (MCP), histine kinase (CheA) and signal

transduction protein (CheW).[20] Alkane sensitive bacteria possess various MCP-encoding genes to interact with extracellular alkane molecules. In *Pseudomonas putida* GPo1, *alkN* gene has been found to encode an MCP for alkane collection.[21] The *tlpS* gene, located downstream of *alkB1*, is believed to encode the MCP in *Pseudomonas aeruginosa* PAO1 for hexadecane accumulation.[22] *Acinetobacter baylyi* ADP1 exhibits strong selection and accumulation towards alkanes.[23-25] The fimbriae on the membrane surface of *Acinetobacter* cells drive them to access alkane droplets to activate alkane hydroxylase AlkM for further degradation.[23-25] The emulsan-coding *wee* gene cluster in *Acinetobacter* contributes to the bacterial emulsification of alkane molecules when attaching on alkane droplets.[26] Uneven distributions of cations usually associate with alkane contamination, resulting in extra cationic strengths on the bioavailability of alkanes in bacterial cells. Therefore, this needs to be considered for its influence on bacterial accumulation of alkanes.

Conventional methods that are used to study bacterial accumulation behaviours include swarm plates,[27] capillary assays,[28] temporal stimulation of tethered cells[29] and automated tracking of swimming cells.[30] They are useful methods to study bacterial movements towards specific chemicals, but require longstanding and labour-intensive pre-treatment work. Raman micro-spectroscopy is widely used in biological studies.[31] As a fast, reproducible and non-destructive approach providing vibrational information of biomolecules, it has been applied to investigate bacterial responses to their surrounding environments.[32,33] Spectral alterations in Raman peaks allow the measurement of cationic effects on bacterial selection and accumulation for alkane molecules.

To our knowledge, this is the first study to use Raman spectral assays to gather information on how nutrients affect the bioavailability of alkanes and alkane mixtures. We used Raman micro-spectroscopy to identify the influences of four cations (Na, K, Mg, Ca) on the selection and

accumulation of alkanes around or inside *A. baylyi* cells. We demonstrated that the bioavailable fraction of alkanes is highly specific to external cations on oil contaminated sites, and the stability of bacterial accumulation towards alkanes is measurable by Raman spectral assay. This method contributes to the deep understanding of changes in bacterial behaviours with different environmental conditions, and has the potential as a tool for the risk assessment of environmental contaminants.

2. Materials and methods

2.1 Bacterial strain and growth conditions

An alkane sensitive bacterial strain *Acinetobacter baylyi* ADP1 was used for all treatments in this study. This strain was inoculated in minimal medium with 20 mM sodium succinate as the sole carbon source, shaking at 150 rpm and 30°C for 16 h. To prepare 1.0 L mineral medium, 1.0 g of $(NH_4)_2SO_4$, 2.5 g of KH_2PO_4, 0.1 g of $MgSO_4 \cdot 7H_2O$, 0.005 g of $FeSO_4 \cdot 7H_2O$, 0.25 g of nitrilotriacetic acid, 0.55 g of NaOH and 1 mL of Bauchop and Elsden solution were mixed well in 1.0 L deionized water and autoclaved.[34] Once harvested by centrifugation at 4000 rpm for 4 min, the cell pellets were washed three times with sterile deionized water and finally re-suspended in fresh mineral medium for use in the experiments. Unless stated otherwise, all chemicals in this study were of analytical grade and purchased from Sigma Aldrich (UK).

2.2 Alkane exposure experiment

Seven pure alkanes (decane, dodecane, tetradecane, hexadecane, nonadecane, eicosane and tetracosane), and mineral oil were selected as the classic alkane mixture. They were dissolved in dimethyl sulfoxide (DMSO) to prepare the 10 g/L stock solution. To investigate the impacts of Na^+, K^+, Mg^{2+} and Ca^{2+} on bacterial selections and accumulations towards alkanes, four cation-

providing chemicals (NaCl, KCl, $MgCl_2$ and $CaCl_2$) were dissolved in mineral medium to prepare 100 mM stock solutions, respectively.

Bacterial suspensions (9 mL) were mixed with 1 mL mineral medium or cation stock solution to reach a final cationic concentration of 10 mM. The alkane stock solution was mixed with bacterial suspensions with or without extra cations to reach a final concentration of 100 mg/L. All the samples were incubated at 30°C for 1 h, and further centrifuged at 5,000 rpm for 5 min to remove the medium. The cell pellets were re-suspended in deionized water and washed three times.

2.3 Capillary assay of alkane chemotaxis

To confirm bacterial selections and accumulations towards alkanes, capillary assays were performed based on the protocol of Li et al. with certain modifications.[32] Capillary tubes (internal diameter of 0.2 mm and length of 10 cm) were immersed into 1 mL of chemotaxis attractant stock solution (alkanes or mineral oil) for 10 min until the liquid was drawn up to ~1 cm of the length of the tube. The capillary was then inserted into the bacterial suspensions and incubated for 1 h at 30°C.

Quantitative polymerase chain reaction (qPCR) was introduced to quantify the 16S rRNA copy numbers of chemotactic bacteria in triplicate. After 1-h incubation, the capillary tube was removed and the 1-cm exterior from the open end was directly plunged into qPCR buffer. The 10 μL qPCR buffer included 1 μL of primer 314F (5'-CCTACGGGNGGCWGCAG-3'), 1 μL of primer 802R (5'-TACNVGGGTATCTAATCC-3'), 3 μL molecular water and 5 μL iTaq™ Universal SYBR® Green Supermix (BioRad, USA). The qPCR thermos cycling program of 16S rRNA was: initial denaturation at 94°C for 3 min; 34 amplification cycles of 94°C for 45 s, 52°C for 45 s, 72°C for 45 s, and fluorescence data acquisition at 80ºC for 15 s. The standard curves were obtained with

serial dilutions of quantified plasmid DNA containing the fragment of 16S rRNA.[35]

2.4 Raman micro-spectroscopy measurement

Prior to Raman micro-spectroscopy measurement, 10 µL of washed cell pellets were transferred onto an aluminium foil coated slide and air-dried at room temperature in a fume cupboard. Raman spectra of all the samples were obtained using an InVia confocal micro-Raman system (Renishaw, Gloucestershire, UK). This system was equipped with a 100 mW 785 nm excitation laser diode. The entrance slit of the spectrometer was 50 µm combined with a 1200 lines per mm (1 cm^{-1} spatial resolution) diffraction grating, allowing the dispersion of Raman signals onto a Master Renishaw Pelletier cooled charged couple detector (CCD). Locations of sample detection were visualized via an attached microscope (Leica Microsystems, Milton Keynes, UK) with ×50 objective (0.75 numerical aperture; ≈1 µm spatial resolution). The Raman system was calibrated using a Renishaw silicon calibration source for wavenumber shifts before sample analysis. All sample spectra were obtained using 50% laser power (13 mW at sample), 10 s acquisition time, and one accumulation within a spectral range from 800 to 2000 cm^{-1}. All treatments were carried out in triplicate, and at least twenty replicates were performed and analysed for each sample.

2.5 Computational analysis of Raman spectra

Unless specifically stated otherwise, all the Raman spectral data were analyzed using the IRootLab toolbox for MatLab (version R2013b, MathWorks, USA).[36] Baseline correction and vector normalization was applied before principal component analysis (PCA) and linear discriminant analysis (LDA). PCA was employed to reduce the dimensionality of the multivariate data and allow the visualization of the natural variance within the data set. To accomplish inter-class separation and minimize intra-class differences, LDA was used to extract inter-category

discriminating features. The separation of individual spectral categories from negative control and pure alkane classes was measured by exporting PCA-derived data. Post-exposure to different types of alkanes or treated with different extra ions, the dispersion of individual Raman spectra to that of negative controls (no alkanes and no extra ions added) and pure alkane was calculated on the values of principal component 1 (PC1) and PC2, and visualized as dispersion indicator (D_I) score plots (see the Supporting Information (SI) for calculation details). In D_I score plots, the increasing D_I value between two categories is proportional to dissimilarity (i.e. higher values indicate greater dissimilarity from controls). The description and transformation of PCA data of each treatment were completed using Python (Version 3.0) (see the SI for the relevant code).

3. Results and discussion

3.1 Raman spectral characterization of alkane exposed A. baylyi

Raman spectra characterized the peaks of pure alkanes and alkane mixture. Since decane, dodecane, tetradecane, hexadecane, nonadecane, eicosane and tetracosane were from the group of linear alkanes, major peaks in their Raman spectra were caused by similar chemical bonds (Figure1). In Figure S1 and Table 1, notable peaks observed in all Raman spectra of n-alkane molecules included 890 cm^{-1} (CH_3 rock), 1060 cm^{-1} (C–C symmetric stretching), 1079 cm^{-1} (C–C stretching), 1136 cm^{-1} (CH_2 stretching), 1296 cm^{-1} (CH_2 twisting) and 1436 cm^{-1} (CH_2 bending).[37] Although Raman spectra of pure n-alkane molecules were similar, spectra of decane and hexadecane showed specific peaks at 1535 cm^{-1}, which might be attributed to the linkages of C and H deformation.[38] In the spectrum of dodecane, two distinct peaks at 961 and 1033 cm^{-1} were assigned to CH_2 rock.[39] Because of the solid state of nonadecane, eicosane and tetracosane, CH_2 bending band shifted to 1440 and 1463 cm^{-1}, indicating an increase in intermolecular interactions and vibrational motion.[40] In the alkane mixture, Raman spectra of mineral oil showed similar peaks at 890, 1060, 1136 and

1436 cm^{-1} (Figure 1H).

To study spectral alterations of alkane exposed bacteria, Raman spectra of original *A. baylyi* were measured as control. Raman peaks at 1238 and 1311 cm^{-1} were assigned to amino acids, and the band of 1441 cm^{-1} was generated from the glycine in bacterial cells (Table 1).[41] The band at 1002 cm^{-1} represents phenylalanine, and the peak at 1663 cm^{-1} was attributed to the protein on cell membranes.[42] *Acinetobacter baylyi* ADP1 are ubiquitous bacteria observed in natural soil environments. They are frequently found to be able to utilize alkanes with carbon lengths ranging from 12 up to 36.[13] Previous work has shown the strong accumulation towards dodecane and tetradecane in *A. baylyi* cells.[35] As a consequence, Raman micro-spectroscopy is able to test the bacterial selections and accumulations towards short-, medium- and long-chain n-alkanes.

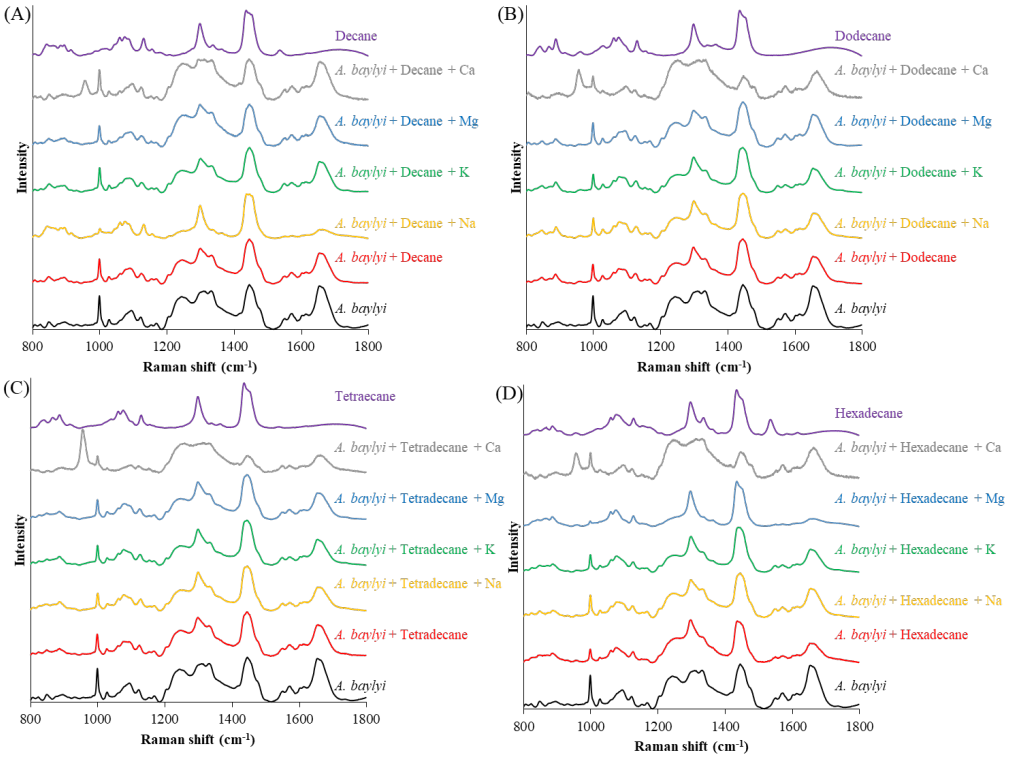

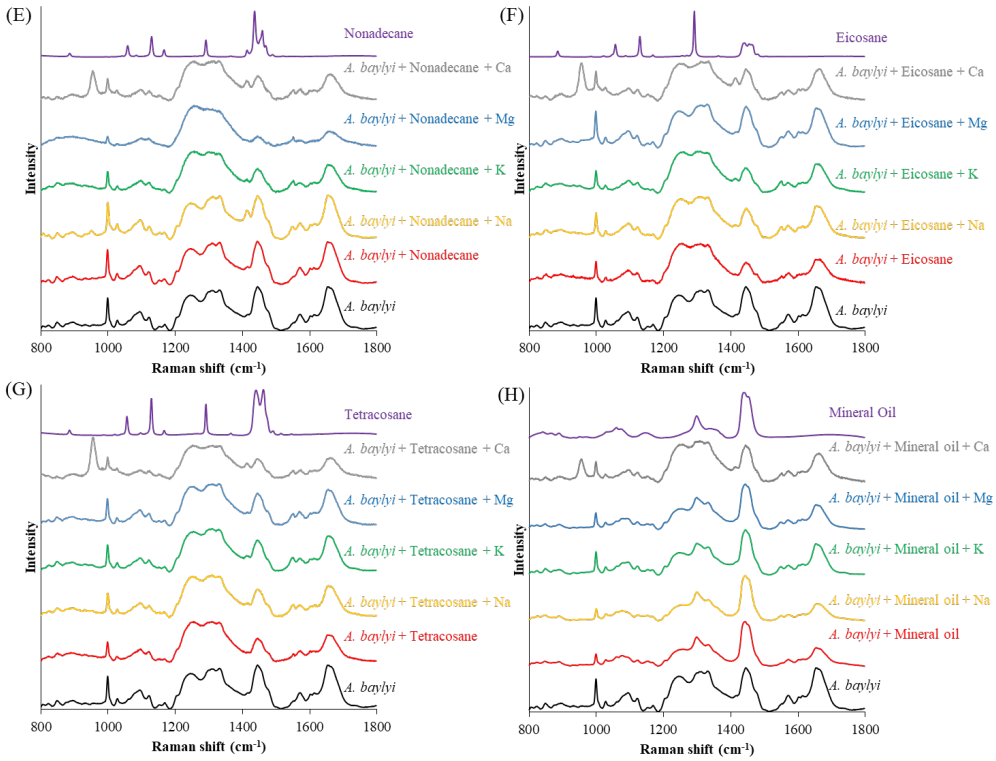

Figure 1. Raman spectra of *A. baylyi* towards decane (A), dodecane (B), tetradecane (C), hexadecane (D), nonadecane (E), eicosane (F), tetracosane (G), and mineral oil (H). Spectra in black are for pure bacterial cells, red for the exposure of alkane, yellow for the treatment with extra sodium, green for the extra potassium, blue for the extra magnesium, grey for the extra calcium and purple for pure alkane.

Post-exposure to decane, dodecane, tetradecane, hexadecane and mineral oil, Raman spectral alterations at 1296 and 1436 cm^{-1} generated from alkanes indicated their accumulation around/inside bacterial cells. However, no significant Raman alterations from alkanes were found in the spectra of nonadecane, eicosane or tetracosane exposures. Sensitive sensing behaviours of *A. baylyi* enabled the accumulation of alkane molecules in/on bacterial cells towards decane to hexadecane, whereas no positive response was found for nonadecane, eicosane and tetracosane. *Acinetobacter* can move towards the area where alkane molecules were available.[12] Once adhering

199 to the alkane droplets, *Acinetobacter* excretes bio-surfactants to emulsify alkane molecules on
200 membranes within a second, contributing to the massive accumulation of molecules on or inside
201 bacterial cells.[43-45]

202 In Figure S2, the accumulation of 16S rRNA copies in capillary tubes of alkane were less than 19
203 carbons range from 8.8×10^{9} to 2.33×10^{11} copies per capillary, significantly higher than those in
204 the treatments of nonadecane, eicosane and tetracosane. Higher copies illustrated the more
205 bioavailable alkanes in capillary tubes for *A. baylyi* to collect. The results from capillary assays
206 confirmed the bioavailability of alkane was related to the bacterial accumulation.

207 **Table 1.** Variations and assignments of Raman bands of alkanes and *A. baylyi*

Band (cm^{-1})	**Tentative bands assignment**	**Origin**
890	Terminal methyl CH_3 rock	All alkanes
1060	C-C symmetric stretch	All alkanes
1079	C-C stretch	All alkanes
1136	CH_2 stretch	All alkanes
1296	CH_2 twist	All alkanes
1436	CH_2 bend	All alkanes
1535	C-H deformation	Decane and Hexadecane
961	CH_2 rock	Dodecane
1033	CH_2 rock	Dodecane

1440	CH_2 bend shift	Nonadecane, eicosane and tetracosane
1463	CH_2 bend shift	Nonadecane, eicosane and tetracosane
1002	Benzene ring breathing	Bacterial phenylalanine
1238	/	Bacterial amino acids
1311	/	Bacterial amino acids
1441	Deformations of CH_2	Bacterial glycine
1663	C=C stretching	Bacterial proteins

208 *3.2 Unstable bioavailability of alkanes*

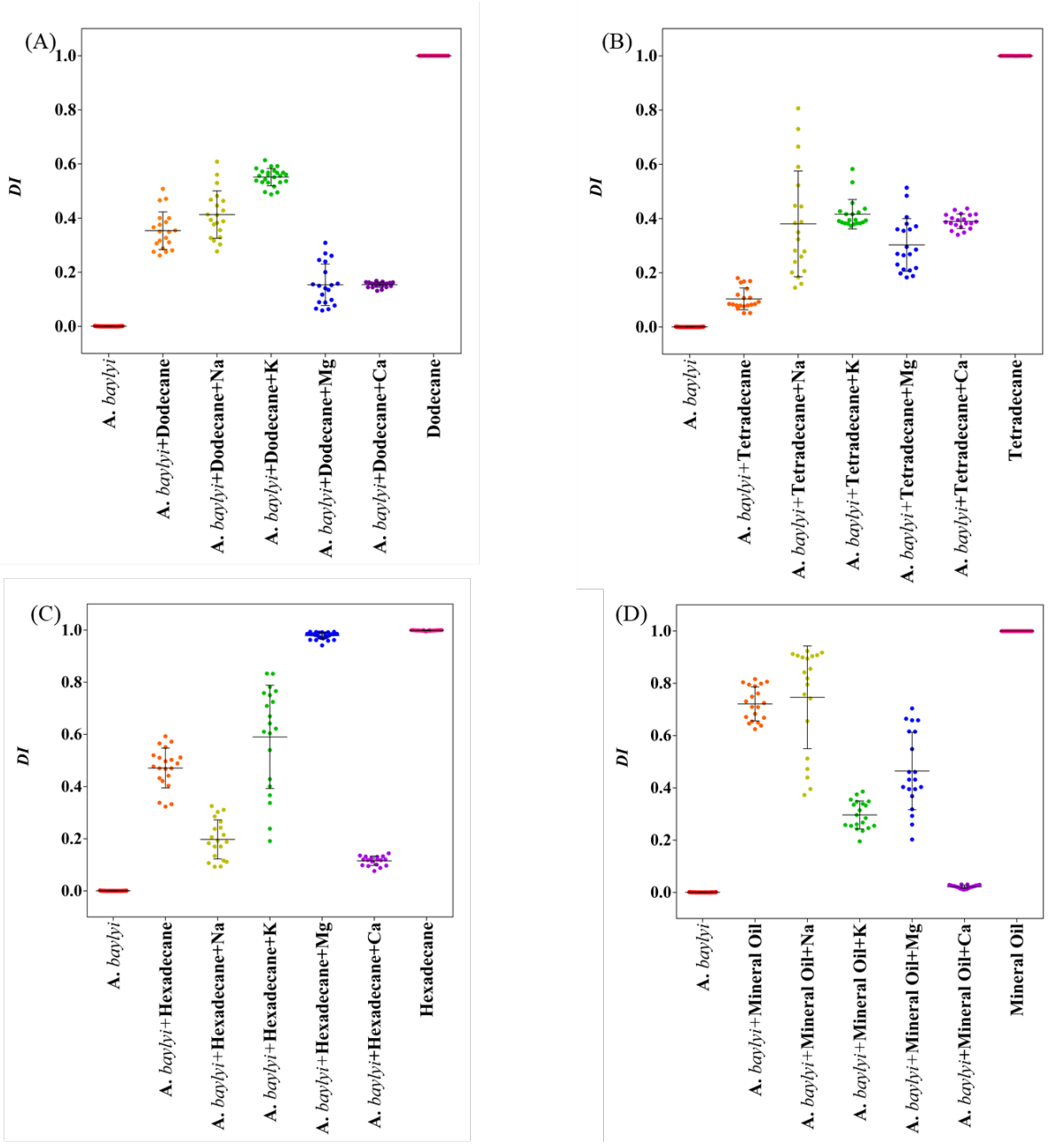

209

210 **Figure 2.** D_I scores of the effects of four nutrient cations on bacterial selections and accumulations

211 of *A. baylyi* towards dodecane (A), tetradecane (B), hexadecane (C), and mineral oil (D)

212

Post-exposed to decane in each treatment, Raman spectra showed distinguishable peak alterations, resulting in significant differences in D_I score plots (Figure S3A). In original MM, the 0.177 D_I value indicated the moderate bacterial accumulation towards decane in *A. baylyi*. In the treatment with Na, D_I values were close to that of pure decane, demonstrating the remarkable enhancement for its accumulation in *A. baylyi*. In contrast, the low D_I values found in K (0.114), Mg (0.066) and Ca (0.012) treatments indicated the decreased bioavailability of decane. The accumulation of decane in *A. baylyi* generated relevant Raman alterations at 1296 and 1436 cm^{-1} in corresponding spectra (Figure 1A). The outer-membrane protein OmpS is responsible for the signal transport of short-chain alkanes such as octane, nonane and decane in bacterial cells.[20] Extra Na in the ambient environment around bacteria may accelerate the signal transport inside cytoplasma, or enhance the emulsification of decane molecules on the cell membrane to increase its bioavailability. Post-exposed to dodecane, D_I values of Na (0.501) or K (0.583) were higher than those in the original MM (0.423), showing the increased bioavailability in *A.baylyi* with these two cations (Figure 2A). It is reported that *A. baylyi* is able to grow with dodecane as the sole carbon source in liquid medium.[46] The strong bacterial affinity of dodecane results in the fast molecules' transport through the cell of *A. baylyi*, which is well characterized by Raman spectra.[32]

From the results in Figure 2B, all tested cations improved the bioavailability of tetradecane, and peak alterations at 1060, 1079 and 1296 cm^{-1} observed in Raman spectra also proved the accumulation of tetradecane in *A. baylyi* cells (Figure 1C). The bioavailable fraction of tetradecane affects the signal transmitter protein, OmpS, and the alkane uptake protein, OmpW in bacterial cells to change their behaviours.[20,47] Extra cations possibly induced more available alkane molecules for bacteria to enhance their upregulations of relevant proteins. The D_I value of bioaccumulated hexadecane in normal MM was 0.547 (Figure 2C), demonstrating its stronger

bacterial affinity compared to tetradecane. In four cation treatments, D_I values were in the order: Mg (0.991) > K (0.788) > Na (0.272) > Ca (0.133). The bioavailability of hexadecane for *A. baylyi* was increased by K and Mg, but decreased by Na and Ca, compared to that in normal MM (Figure 2C). Due to the influences of cations, the incremental/reduced available fraction of hexadecane regulates its accumulation in *Acinetobacter*,[48,49] and possibly affects the expression of relevant sensory proteins at cellular level.[50]

In normal and extra Na equipped MM, the accumulation of *A. baylyi* towards nonadecane was weak, proved by the relatively low D_I values, 0.001 and 0.002, respectively (Figure S3B). The presence of extra K, Mg and Ca slightly increased the bioavailability of nonadecane, but no major alterations were found in relevant Raman spectra (Figure 1E and 2E), indicating that only small amounts of nonadecane molecules were accumulated by *A. baylyi*. Eicosane and tetracosane had similar D_I values in normal medium (Figure S3C and S3D), demonstrating their weak bioavailability. The four tested cations were limited in changing the available fractions of eicosane and tetracosane, and their effects on the accumulation behaviour of *A.baylyi* were slight. Although the uptake and degradation of long-chain alkanes in *Acinetobacter* is well-documented,[51] further studies are required to understand how their bioavailability and bioaccumulation in different environmental conditions impact ecological systems. Different from short and medium chain alkanes, nonadecane, eicosane and tetracosane are waxy solids at room temperature and atmospheric pressure. In the liquid medium, the low solubility of long chain alkane limits the interaction with cations. Therefore, compared with liquid alkanes, their bioavailable fractions remain at a relatively low level with extra cations.

The D_I results in Figure 2D indicated the strong bioavailability of mineral oil. The similar D_I value found in Na treatment demonstrated the weak effect on its accumulation in *A. baylyi* cells.

Although the bioavailability was reduced with K and Mg, the Raman peak at 1296 cm^{-1} (CH_2 twisting of mineral oil molecule) was observed in relevant spectra, showing its substantial bioaccumulation (Figure 1G). However, the extra Ca significantly reduced the bioavailability of mineral oil, leading to the unchanged Raman spectra pre- and post-exposed to mineral oil (Figure 1G and 2D). As a mixture of different alkanes, mineral oil has strong bioavailability for bacteria. Also, extra cations can affect various components in mineral oil, resulting in the instability of bioavailable mineral oil. Therefore, by evaluating the stability of bioavailable hydrocarbons, the Raman spectral assay provides a tool for the risk assessment of oil contamination.

3.3 Impacts of cations on alkane bioaccumulation

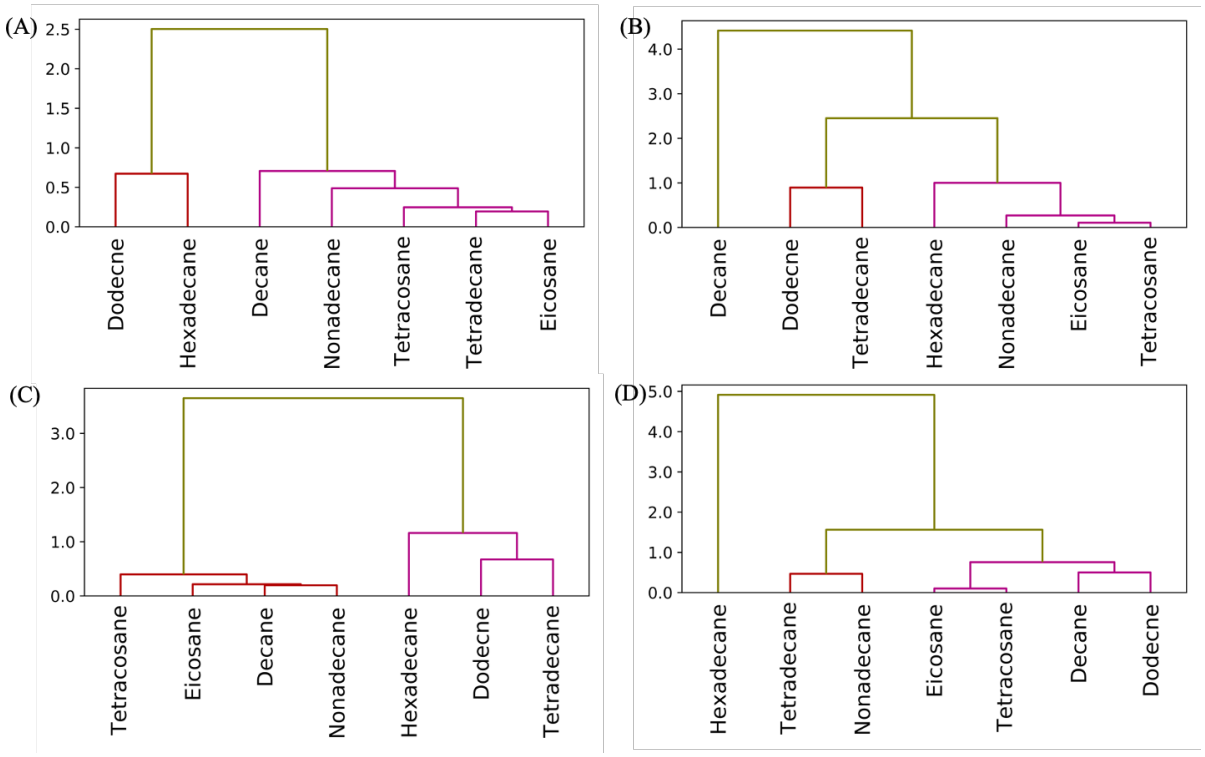

Figure 3. Hierarchy clustering analysis for the bioaccumulation of *A. baylyi* towards alkanes in the normal medium (A), with extra Na (B), K (C), and Mg (D). Dendrograms represent alkanes

cluster, and y axis indicates the differences in bioavailability of alkanes (high value demonstrates great dissimilarity).

From the results in Figure 3, extra cations exhibited different influences on the bioavailability of short chain (decane and dodecane), medium chain (tetradecane, hexadecane and nonadecane), and long chain alkane (eicosane and tetracosane). In the normal medium, dodecane and hexadecane from one cluster indicated their adequate available fractions for bacteria to access (Figure 3A), but the noticeable variations demonstrated the diverse bacterial accumulations towards these two alkanes (Figure S4A). The strong selections and accumulations towards dodecane and hexadecane are attributed to the emulsan produced from *Acinetobacter* to improve the bacterial emulsification, and then increase the accumulation of alkane molecules.[26,52]

In the Na treatment, the highest impact factor (0.89) and tiny variations of decane-exposed bacterial cells reflected its stable bioavailable fraction for bacterial cells to collect (Figure 4 and Figure S4B). The sole cluster of decane in the dendrogram also indicated the specific effect of sodium on the bioaccumulation of this alkane (Figure 3B). Dodecane and tetradecane fell in one cluster, showing the positive response of *A. baylyi* towards these two alkanes (Figure 3B). Owing to the high halotolerant ability of *A. baylyi*, we believe that this bacterial strain is sensitive to the change in the concentration of Na in its surrounding environments.[34] The increase in external Na concentration affects the bacterial adherence and emulsification ability, leading to the uneven bioaccumulation of alkane molecules on/inside cell membranes,[53] which is also indicated by the significant variations of dodecane, tetradecane and hexadecane.

Alkane clusters in Figure 3C illustrated two different ways that K influenced the bioavailability of alkanes. The positive effect of extra K on bacterial selections and accumulations towards dodecane, tetradecane and hexadecane contributed to high D_I values: 0.583, 0.416 and 0.788, respectively

(Figure S4C). The bioavailability of the other 4 tested alkanes was weakly related to the impact of K, proved by the factor shown in Figure 5. The external K enhanced the bacterial accumulation of medium-chain n-alkanes,[54] and improved the transfer of information signals among bacterial cells to collect available alkane molecules.[55] The bioaccumulation of dodecane by *A. baylyi* increased smoothly, but bioavailable tetradecane and hexadecane molecules were not well-distributed in the medium with extra K, as shown by the noticeable variations of these two alkanes. As a consequence, K is essential for bacteria to accumulate alkane molecules, and can also influence the heterogeneity of bioavailable alkanes' distribution.

The dendrogram illustrated the positive relation of medium-chain alkane including dodecane, tetradecane and hexadecane to Mg (Figure 3D). The highest D_I score was from hexadecane, showing its strong bioaccumulation in *A. baylyi*, and the small variation proves that extra Mg was able to stabilize the bioavailability of this alkane. The bioavailability of tetradecane and nonadecane was also strongly correlated to the effect from external Mg (Figure 4). Extracellular Mg stabilized the bioaccumulation of *A. baylyi* towards tetradecane, hexadecane and nonadecane.[56] However, D_I values in Figure S4D showed that the impacts of Mg on the bioavailability were not uniform for all n-alkanes. Hence, we deduce that the transportation proteins of hexadecane in *A. baylyi* are more likely to interact with Mg than that of other n-alkanes.

The low D_I values indicated that extra Ca significantly reduce the bioavailability of alkanes (Figure S4E). The limited bacterial accumulations towards n-alkanes also resulted in the low impact factor of Ca in Figure 5. A more than 100 nM concentration of extracellular Ca can prohibit bacterial movements,[57] and bacterial cells tend to aggregate by interacting with the anionic components in bacterial cells.[58] Successful bacterial accumulation requires the efficient movement towards specific molecules, but extra Ca disables such ability of bacteria. External Ca possibly blocks

318 transferring channels of alkanes' signals in bacterial cells, leading to the inactive bioaccumulation
319 of them.

320 We investigated impact factors of cations that account for the alkanes' bioaccumulation, and
321 compared them with those in the normal medium. The heatmap from hierarchy clustering analysis
322 (Figure 5), shows the specific accumulation behaviour of *A. baylyi* towards alkanes is attributed to
323 different impacts from each cation. The bioavailability of decane and hexadecane is highly
324 sensitive to extra Na and Mg, respectively. Bioavailable fractions of dode-, tetra- and hexadecane
325 are increased for bacteria to accumulate with external K. Because of cationic impacts, bacterial
326 activities cannot remain at stable levels, especially on oil contaminated sites that involve
327 complicated physicochemical conditions. Therefore, with the help of Raman micro-spectroscopy,
328 we were able to visualize the effects of cations on bacteria, to uncover the underlying limitations
329 to bacterial remediation of oil contaminated sites. Although further studies are required before
330 applying this instrument in real environmental conditions, this method has already provided
331 positive results in this study, to indicate it can help improve bioremediation of oil contamination.

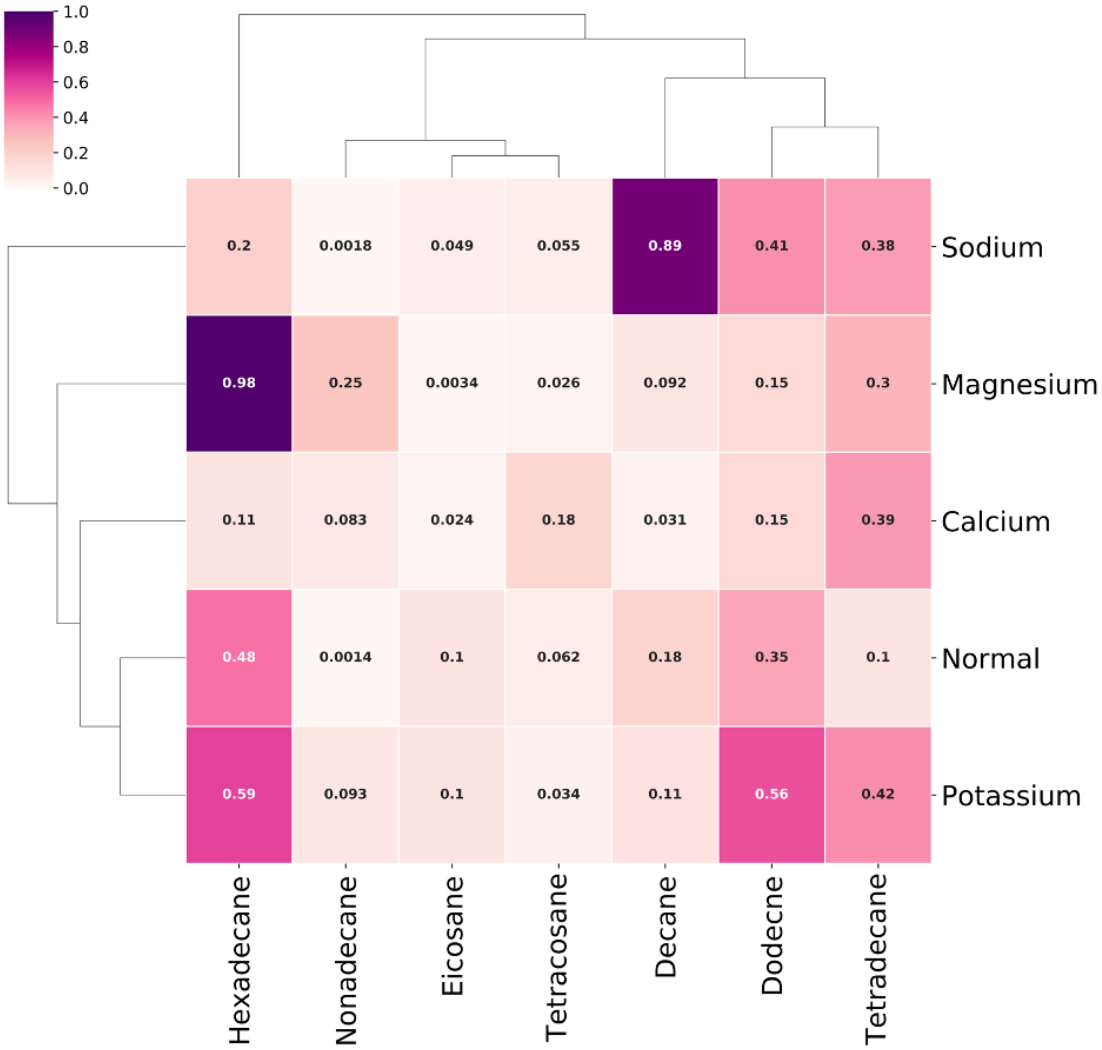

332

333 **Figure 4.** Cluster heatmap for the accumulation behaviours of *A. baylyi* with different cations. The

334 impact factor of the cation was characterized into five quartiles, and is illustrated with intensity.

335 The dendrogram on the left represents cation clusters, and the one on the top refers to the alkane

336 clusters.

337 *3.4 Cationic effects on bacterial accumulation in alkane mixture*

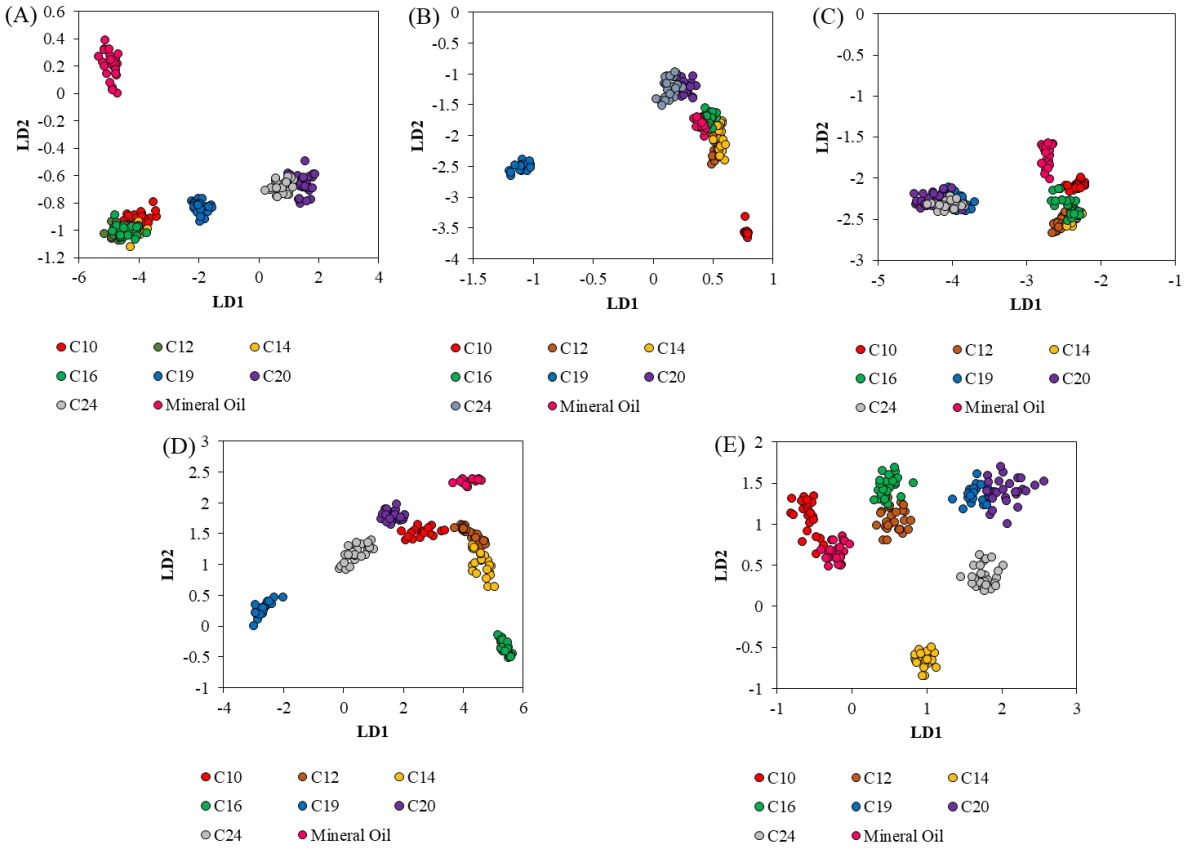

338

339 **Figure 5.** LDA plots of alkane chemotactic selection of *A. baylyi* in alkane mixture (mineral oil)
340 with no extra ions (A), and in the presence of Na (B), K (C), Mg (D), and Ca (E)

341 The PCA-LDA of Raman spectra was performed to determine the available components in the
342 mineral oil for bacterial cells to interact with. In normal MM, the majority of alkane molecules
343 collected by *A. baylyi* in mineral oil were mainly short- and medium-chain alkanes, including
344 decane, dodecane, tetradecane and hexadecane (Figure 5A). Although mineral oil consists of
345 alkane molecules from C_{10} to C_{35},[59] the major components in its bioavailable fraction are short-
346 and medium-chain n-alkanes.

347 Extra Na enabled the LDA group of mineral oil aggregates with dodecane, tetradecane and

hexadecane in LDA plot (Figure 5B), indicating the increased bacterial accumulation of these three alkanes in alkane mixture.[53] D_1 scores also confirmed that extra Na prompts the bioavailability of carbon lengths of 12, 14 and 16. The LD1 values of Raman spectra indicated that external K enabled *A. baylyi* to capture large amounts of decane and hexadecane molecules in mineral oil (Figure 5C). Tetradecane exhibited strong affinity to *A. baylyi* with extra K as well. Hence, K may accelerate the movement of *A. baylyi* towards decane and hexadecane molecules, but reduce the accumulation of other n-alkanes in mineral oil.[54] The close distance of LDA groups indicated a number of dodecane molecules accumulated by *A. baylyi* in mineral oil with extra Mg (Figure 5D). Since extra Mg is able to stabilize the phosphorylated CheY, it can assist bacterial cells to access chemical molecules faster in alkane mixture.[60] From the LDA in Figure 5E, Ca weakened bacterial accumulation behaviours towards alkane molecules in mineral oil. Unlike the LDA plot of the normal medium, separated LDA groups of pure n-alkanes demonstrated the limited bacterial movement and reduce bioavailability of mineral oil due to extra Ca in aquatic environments.

Mineral oil is a complex alkane mixture comprising saturated n-alkanes and aromatic hydrocarbons.[59] Diverse cations challenge the bacterial accumulation of alkane molecules and affect their bioavailability, leading to complex impacts on ecological systems.[61,62] Therefore, the impacts of cations on the bioavailability of alkanes are significant for the treatment of oil contamination. Raman micro-spectroscopy has been used successfully to measure chemotaxis-related behaviours of *A .baylyi* towards hydrocarbons.[32] This application confirms that extra cations can change the dominant components in alkane mixture, thereby leading to different accumulation behaviours of bacteria towards alkane molecules in alkane mixtures.

This study applied Raman micro-spectroscopy to investigate the impacts of nutrient cations on the bioavailability of alkanes and alkane mixture in the liquid phase. To the best of our knowledge,

this is the first study to use Raman spectral methods to show the bacterial selections and accumulations of alkanes under different environmental conditions. The cation-alkane patterns observed the unstable/variable bioavailability of alkanes in the presence of extra cations, and differentiated bacterial accumulation behaviours in complex environments. Varying physicochemical conditions disturb the stable response of bacteria towards hydrocarbons. Therefore, this study provides a new perspective and method to gain information on the change in bioavailability of alkanes for the potential treatment of oil contamination incidents. Further work is required to elucidate the combining effects of nutrients for bacterial accumulation of hydrocarbons in environmental samples from oil-contaminated sites. In the future, this Raman spectral assay is helpful to evaluate the bioavailability and biotoxicity of environmental pollutants in natural ecological systems.

Acknowledgements

The authors would like to thank Lancaster University FST Research Grant for financial support. HL was supported by the China Scholarship Council (CSC) and Postdoctoral Fund of Jiangsu Province.

References

1. Bence, A.; Kvenvolden, K.; Kennicutt, M., Organic geochemistry applied to environmental assessments of Prince William Sound, Alaska, after the Exxon Valdez oil spill—a review. *Org. Geochem.* **1996,** *24* (1), 7-42.

2. Bragg, J. R.; Prince, R. C.; Harner, E. J.; Atlas, R. M., Effectiveness of bioremediation for the Exxon Valdez oil spill. *Nature* **1994,** *368* (6470), 413-418.

3. Camilli, R.; Reddy, C. M.; Yoerger, D. R.; Van Mooy, B. A.; Jakuba, M. V.; Kinsey, J. C.; McIntyre, C. P.; Sylva, S. P.; Maloney, J. V., Tracking hydrocarbon plume transport and biodegradation at Deepwater Horizon. *Science* **2010,** *330* (6001), 201-204.

4. Zhang, D.; Ding, A.; Cui, S.; Hu, C.; Thornton, S. F.; Dou, J.; Sun, Y.; Huang, W. E., Whole cell bioreporter application for rapid detection and evaluation of crude oil spill in seawater caused by Dalian oil tank explosion. *Water Res.* **2013,** *47* (3), 1191-1200.

5. Wang, C.; Shi, X.; Li, W.; Wang, L.; Zhang, J.; Yang, C.; Wang, Z., Oil species identification technique developed by Gabor wavelet analysis and support vector machine based on concentration-synchronous-matrix-fluorescence spectroscopy. *Mar. Pollut. Bull.* **2016**, *104* (1-2), 322-328.

6. Peterson, C. H.; Rice, S. D.; Short, J. W.; Esler, D.; Bodkin, J. L.; Ballachey, B. E.; Irons, D. B., Long-term ecosystem response to the Exxon Valdez oil spill. *Science* **2003,** *302* (5653), 2082-2086.

7. Piatt, J. F.; Lensink, C. J.; Butler, W.; Kendziorek, M.; Nysewander, D. R., Immediate impact of the'Exxon Valdez'oil spill on marine birds. *The Auk.* **1990**, *107*, 387-397.

8. Wang, Z.; Fingas, M. F., Development of oil hydrocarbon fingerprinting and identification techniques. *Mar. Pollut. Bull.* **2003,** *47* (9–12), 423-452.

9. Sticher, P.; Jaspers, M.; Stemmler, K.; Harms, H.; Zehnder, A.; Van Der Meer, J. R., Development and characterization of a whole-cell bioluminescent sensor for bioavailable middle-chain alkanes in contaminated groundwater samples. *Appl. Environ. Microb.* **1997,** *63* (10), 4053-4060.

10. Van Beilen, J.; Li, Z.; Duetz, W.; Smits, T.; Witholt, B., Diversity of alkane hydroxylase systems in the environment. *Oil Gas Sci. Technol.* **2003,** *58* (4), 427-440.

11. Van Beilen, J. B.; Funhoff, E. G., Alkane hydroxylases involved in microbial alkane degradation. *Appl. Microbiol. Biotechnol.* **2007,** *74* (1), 13-21.

12. Wentzel, A.; Ellingsen, T. E.; Kotlar, H.-K.; Zotchev, S. B.; Throne-Holst, M., Bacterial metabolism of long-chain n-alkanes. *Appl. Microbiol. Biotechnol.* **2007,** *76* (6), 1209-1221.

13. Zhang, D.; He, Y.; Wang, Y.; Wang, H.; Wu, L.; Aries, E.; Huang, W. E., Whole‐cell bacterial bioreporter for actively searching and sensing of alkanes and oil spills. *Microb. Biotechnol.* **2012,** *5* (1), 87-97.

14. Leahy, J. G.; Colwell, R. R., Microbial degradation of hydrocarbons in the environment. *Microbiol. Rev.* **1990,** *54* (3), 305-315.

15. Yakimov, M. M.; Timmis, K. N.; Golyshin, P. N., Obligate oil-degrading marine bacteria. *Curr. Opin. Biotech.* **2007,** *18* (3), 257-266.

16. Annweiler, E.; Materna, A.; Safinowski, M.; Kappler, A.; Richnow, H. H.; Michaelis, W.; Meckenstock, R. U., Anaerobic degradation of 2-methylnaphthalene by a sulfate-reducing enrichment culture. *Appl. Environ. Microb.* **2000,** *66* (12), 5329-5333.

17. de la Cueva, S. C.; Rodríguez, C. H.; Cruz, N. O. S.; Contreras, J. A. R.; Miranda, J. L., Changes in bacterial populations during bioremediation of soil contaminated with petroleum hydrocarbons. *Water Air Soil Poll.* **2016,** *227* (3), 91.

18. Shao, Z.; Wang, W., Enzymes and genes involved in aerobic alkane degradation. *Front. Microbiol.* **2013,** *4*, 116.

19. Parales, R. E.; Harwood, C. S., Bacterial chemotaxis to pollutants and plant-derived aromatic molecules. *Curr. Opin. Biotech.* **2002,** *5* (3), 266-273.

20. Wang, W.; Shao, Z., The long-chain alkane metabolism network of Alcanivorax dieselolei. *Nat. Comm.* **2014,** *5*, 5755.

21. van Beilen, J. B.; Panke, S.; Lucchini, S.; Franchini, A. G.; Röthlisberger, M.; Witholt, B., Analysis of Pseudomonas putida alkane-degradation gene clusters and flanking insertion sequences: evolution and regulation of the alk genes. *Microbiology* **2001,** *147* (6), 1621-1630.

22. Smits, T. H.; Witholt, B.; van Beilen, J. B., Functional characterization of genes involved in alkane oxidation by Pseudomonas aeruginosa. *Anton. Leeuw. Int. J. G.* **2003,** *84* (3), 193-200.

23. Huang, W. E.; Singer, A. C.; Spiers, A. J.; Preston, G. M.; Whiteley, A. S., Characterizing the regulation of the Pu promoter in Acinetobacter baylyi ADP1. *Environ. Microbiol.* **2008,** *10* (7), 1668-1680.

24. Vaneechoutte, M.; Young, D. M.; Ornston, L. N.; De Baere, T.; Nemec, A.; Van Der Reijden, T.; Carr, E.; Tjernberg, I.; Dijkshoorn, L., Naturally transformable Acinetobacter sp. strain ADP1 belongs to the newly described species Acinetobacter baylyi. *Appl. Environ. Microb.* **2006,** *72* (1), 932-936.

25. Young, D. M.; Parke, D.; Ornston, L. N., Opportunities for genetic investigation afforded by Acinetobacter baylyi, a nutritionally versatile bacterial species that is highly competent for natural transformation. *Annu. Rev. Microbiol.* **2005,** *59*, 519-551.

26. Kothari, A.; Charrier, M.; Wu, Y.-W.; Malfatti, S.; Zhou, C. E.; Singer, S. W.; Dugan, L.; Mukhopadhyay, A., Transcriptomic analysis of the highly efficient oil-degrading bacterium Acinetobacter venetianus RAG-1 reveals genes important in dodecane uptake and utilization. *FEMS Microbiol. Lett.* **2016,** *363*, (20).

27. Kearns, D. B., A field guide to bacterial swarming motility. *Nat. Rev. Microbiol.* **2010,** *8* (9), 634-44.

28. Berg, H. C.; Turner, L., Chemotaxis of bacteria in glass capillary arrays. Escherichia coli, motility, microchannel plate, and light scattering. *Biophys. J.* **1990,** *58* (4), 919-930.

29. Block, S. M.; Segall, J. E.; Berg, H. C., Adaptation kinetics in bacterial chemotaxis. *J. Bacteriol.* **1983,** *154* (1), 312-323.

30. Shi, L. Z.; Nascimento, J.; Chandsawangbhuwana, C.; Berns, M. W.; Botvinick, E. L., Real-time automated tracking and trapping system for sperm. *Microsc. Res. Techniq.* **2006,** *69* (11), 894-902.

31. Efrima, S.; Zeiri, L., Understanding SERS of bacteria. *J. Raman Spectrosc.* **2009,** *40* (3), 277-288.

32. Li, H.; Martin, F. L.; Zhang, D., Quantification of Chemotaxis-Related Alkane Accumulation in Acinetobacter baylyi Using Raman Microspectroscopy. *Anal. Chem.* **2017,** *89* (7), 3909-3918.

33. Li, H.; Martin, F. L.; Jones, K. C.; Zhang, D., Interrogating the Transient Selectivity of Bacterial Chemotaxis-Driven Affinity and Accumulation of Carbonaceous Substances via Raman Microspectroscopy. *Front. Microbiol.* **2019,** *10*, 2215.

34. Jia, J.; Li, H.; Zong, S.; Jiang, B.; Li, G.; Ejenavi, O.; Zhu, J.; Zhang, D., Magnet bioreporter device for ecological toxicity assessment on heavy metal contamination of coal cinder sites. *Sensor. Actuat. B-Chem.* **2016,** *222*, 290-299.

35. Li, H.; Li, C.; Martin, F. L.; Zhang, D., Diagnose Pathogens in Drinking Water via Magnetic Surface-Enhanced Raman Scattering (SERS) Assay. *Mater. Today: Proceedings* **2017,** *4* (1), 25-31.

36. Trevisan, J.; Angelov, P. P.; Scott, A. D.; Carmichael, P. L.; Martin, F. L., IRootLab: a free and open-source MATLAB toolbox for vibrational biospectroscopy data analysis. *Bioinformatics* **2013,** *29* (8), 1095-1097.

37. Mizushima, S.-i.; Simanouti, T., Raman frequencies of n-paraffin molecules. *J. Am. Chem. Soc.* **1949,** *71* (4), 1320-1324.

38. Sheppard, N.; Simpson, D. M., The infra-red and Raman spectra of hydrocarbons. Part II. Paraffins. *Quarterly Reviews, Chemical Society* **1953,** *7* (1), 19-55.

487 39. Kalyanasundaram, K.; Thomas, J., The conformational state of surfactants in the solid state
488 and in micellar form. A laser-excited Raman scattering study. *J. Phys. Chem.* **1976,** *80* (13), 1462-
489 1473.
490 40. Corsetti, S.; Rabl, T.; McGloin, D.; Kiefer, J., Intermediate phases during solid to liquid
491 transitions in long-chain n-alkanes. *Phys. Chem. Chem. Phys.* **2017,** *19* (21), 13941-13950.
492 41. Cui, L.; Chen, P.; Chen, S.; Yuan, Z.; Yu, C.; Ren, B.; Zhang, K., In situ study of the
493 antibacterial activity and mechanism of action of silver nanoparticles by surface-enhanced Raman
494 spectroscopy. *Anal. Chem.* **2013,** *85* (11), 5436-5443.
495 42. De Gelder, J.; De Gussem, K.; Vandenabeele, P.; Moens, L., Reference database of Raman
496 spectra of biological molecules. *J. Raman Spectrosc.* **2007,** *38* (9), 1133-1147.
497 43. Boulton, C.; Ratledge, C., The physiology of hydrocarbon-utilizing microorganisms.
498 *Topics in enzyme and fermentation biotechnology* **1984,** *9*, 11-77.
499 44. Haferburg, D.; Hommel, R.; Claus, R.; Kleber, H.-P., Extracellular microbial lipids as
500 biosurfactants. In *Bioproducts*, Springer: 1986; pp 53-93.
501 45. Singer, M.; Finnerty, W., Microbial metabolism of straight-chain and branched alkanes. In
502 *Microbial metabolism of straight-chain and branched alkanes*, Macmillan: 1984; pp 1-60.
503 46. Zheng, Y.; Li, L.; Liu, Q.; Qin, W.; Yang, J.; Cao, Y.; Jiang, X.; Zhao, G.; Xian, M.,
504 Boosting the free fatty acid synthesis of Escherichia coli by expression of a cytosolic Acinetobacter
505 baylyi thioesterase. *Biotechnol. Biofuels* **2012,** *5* (1), 76.
506 47. Jung, J.; Jang, I.-a.; Ahn, S.; Shin, B.; Kim, J.; Park, C.; Jee, S. C.; Sung, J.-S.; Park, W.,
507 Molecular mechanisms of enhanced bacterial growth on hexadecane with red clay. *Microb. Ecol.*
508 **2015,** *70* (4), 912-921.
509 48. Rosenberg, M.; Bayer, E. A.; Delarea, J.; Rosenberg, E., Role of thin fimbriae in adherence
510 and growth of Acinetobacter calcoaceticus RAG-1 on hexadecane. *Appl. Environ. Microb.* **1982,**
511 *44*, (4), 929-937.
512 49. Geißdörfer, W.; Kok, R. G.; Ratajczak, A.; Hellingwerf, K. J.; Hillen, W., The genes rubA
513 and rubB for alkane degradation in Acinetobacter sp. strain ADP1 are in an operon with estB,
514 encoding an esterase, andoxyR. *J. Bacteriol.* **1999,** *181* (14), 4292-4298.
515 50. Wang, W.; Shao, Z., Diversity of flavin-binding monooxygenase genes (almA) in marine
516 bacteria capable of degradation long-chain alkanes. *FEMS Microbiol. Ecol.* **2012,** *80* (3), 523-533.

517 51. Sakai, Y.; Maeng, J. H.; Kubota, S.; Tani, A.; Tani, Y.; Kato, N., A non-conventional
518 dissimilation pathway for long chain n-alkanes in Acinetobacter sp. M-1 that starts with a
519 dioxygenase reaction. *J. Ferment. Bioeng.* **1996,** *81* (4), 286-291.
520 52. Rosenberg, E.; Zuckerberg, A.; Rubinovitz, C.; Gutnick, D., Emulsifier of Arthrobacter
521 RAG-1: isolation and emulsifying properties. *Appl. Environ. Microb.* **1979,** *37* (3), 402-408.
522 53. Fernandez-Linares, L.; Acquaviva, M.; Bertrand, J.-C.; Gauthier, M., Effect of sodium
523 chloride concentration on growth and degradation of eicosane by the marine halotolerant
524 bacterium Marinobacter hydrocarbonoclasticus. *Syst. Appl. Microbiol.* **1996,** *19* (1), 113-121.
525 54. Lu, N.; Bevard, T.; Massoudieh, A.; Zhang, C.; Dohnalkova, A. C.; Zilles, J. L.; Nguyen,
526 T. H., Flagella-mediated differences in deposition dynamics for Azotobacter vinelandii in porous
527 media. *Environ. Sci. Technol.* **2013,** *47* (10), 5162-5170.
528 55. Humphries, J.; Xiong, L.; Liu, J.; Prindle, A.; Yuan, F.; Arjes, H. A.; Tsimring, L.; Suel,
529 G. M., Species-Independent Attraction to Biofilms through Electrical Signaling. *Cell* **2017,** *168*
530 (1-2), 200-209.
531 56. Welch, M.; Oosawa, K.; Aizawa, S.-l.; Eisenbach, M., Phosphorylation-dependent binding
532 of a signal molecule to the flagellar switch of bacteria. *P. Natl. Acad. Sci. USA* **1993,** *90* (19),
533 8787-8791.
534 57. Ordal, G. W., Calcium ion regulates chemotactic behaviour in bacteria. *Nature* **1977,** *270*
535 (5632), 66-67.
536 58. Rose, R.; Dibdin, G.; Shellis, R., A quantitative study of calcium binding and aggregation
537 in selected oral bacteria. *J. Dent. Res.* **1993,** *72* (1), 78-84.
538 59. Moret, S.; Scolaro, M.; Barp, L.; Purcaro, G.; Conte, L. S., Microwave assisted
539 saponification (MAS) followed by on-line liquid chromatography (LC)-gas chromatography (GC)
540 for high-throughput and high-sensitivity determination of mineral oil in different cereal-based
541 foodstuffs. *Food Chem.* **2016,** *196*, 50-7.
542 60. Stock, A. M.; Martinez-Hackert, E.; Rasmussen, B. F.; West, A. H.; Stock, J. B.; Ringe,
543 D.; Petsko, G. A., Structure of the magnesium-bound form of CheY and mechanism of phosphoryl
544 transfer in bacterial chemotaxis. *Biochemistry* **1993,** *32* (49), 13375-13380.
545 61. Lal, B.; Khanna, S., Degradation of crude oil by Acinetobacter calcoaceticus and
546 Alcaligenes odorans. *J. Appl. Microbiol.* **1996,** *81* (4), 355-362.

62. Prince, R. C.; McFarlin, K. M.; Butler, J. D.; Febbo, E. J.; Wang, F. C.; Nedwed, T. J., The primary biodegradation of dispersed crude oil in the sea. *Chemosphere* **2013,** *90* (2), 521-526.